

The First O,C,S-Coordinating Pincer-Type Ligand and Its Application to the Synthesis of a Triorganotin Cation Stabilized by Two Different Donor Atoms[†]

Jan Fischer, Markus Schürmann, Michael Mehring, Uwe Zachwieja, and Klaus Jurkschat*

Lehrstuhl für Anorganische Chemie II der Universität Dortmund, D-44221 Dortmund, Germany

Received January 20, 2006

The syntheses and molecular structures of the bromo-substituted triarylphosphane sulfide (3-Br-5-*t*-Bu-C₆H₃)P(S)Ph₂ (**1**), the arylphosphonic acid di-isopropyl ester {3-*t*-Bu-5-[P(S)Ph₂]-C₆H₃}P(O)(O-*i*-Pr)₂ (**2**), its triphenyltin derivative {5-*t*-Bu-3-[P(S)Ph₂]-2-(SnPh₃)-C₆H₂}P(O)(O-*i*-Pr)₂ (**3**), and the corresponding triorganostannylum salt {4-*t*-Bu-2-[P(O)(O-*i*-Pr)₂]-6-[P(S)Ph₂]-C₆H₂}SnPh₂⁺PF₆⁻ (**4**) are reported. By reaction with bromide ion, the latter is converted in situ to the intramolecularly coordinated benzoxaphosphastannole derivative [1(P),3(Sn)-SnPh₂OP(O)(O-*i*-Pr)-6-*t*-Bu-4-P(S)Ph₂]C₆H₂ (**5**). Ab initio MO calculations on the ethoxy-substituted analogue of compound **4** indicate a reduced positive charge at the tin atom in comparison with previously reported {4-*t*-Bu-2,6-[P(O)(OEt)₂]₂C₆H₂}SnPh₂⁺PF₆⁻.

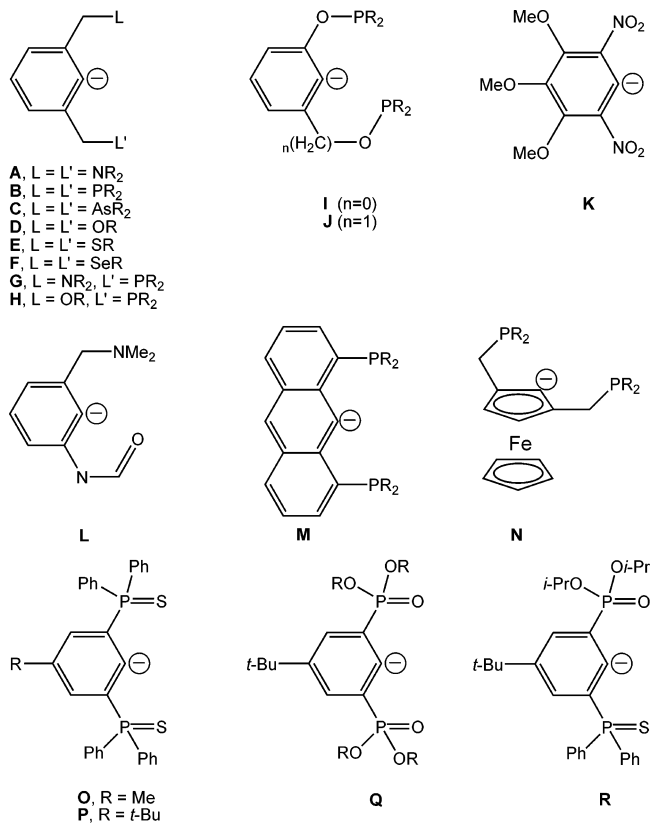
Introduction

Since their first appearance in the late 1970s^{1–3} L,C,L'-coordinating pincer-type ligands of types **A–H** (Chart 1) have become a rather popular class of compounds, the chemistry of which has been thoroughly reviewed.^{4–6} Over the years the classic pincer-type ligands (**A–H**) containing a phenyl backbone and methylene bridges between the donor atoms L, L' and the phenyl ring have been modified and developed further to give ligands containing oxygen (types **I, J**)^{7,8} or nitrogen (types **K, L**)^{9,10} bridges, or anthracene (type **M**)¹¹ and ferrocene^{12,13} (type **N**) backbones, respectively (Chart 1). What makes all these ligands so fascinating is their ability to stabilize metals in unusual oxidation states and to participate, as their metal complexes, in a variety of homogeneously catalyzed organic reactions.^{14–16} In recent years C–H bond activation was also achieved with pincer-type ligand-containing organometallic

[†] Dedicated to Professor Herbert Jacobs on the occasion of his 70th birthday. Part of this work was first presented at the Symposium of the Graduiertenkolleg 352, *Synthetic, Mechanistic and Reaction-Engineering Aspects of Metal-Containing Catalysts*, November 17, 2005, TU Berlin, Germany, Book of Abstracts, p 17.

- (1) Shaw, B. L.; Moulton, C. J. *J. Chem. Soc., Dalton Trans.* **1976**, 1020.
- (2) Shaw, B. L.; Crocker, C.; Errington, R. J.; McDonald, W. S.; Odell, K. J.; Goodfellow, R. J. *J. Chem. Soc., Chem. Commun.* **1979**, 498.
- (3) Shaw, B. L.; Errington, J.; McDonald, W. S. *J. Chem. Soc., Dalton Trans.* **1980**, 2312.
- (4) van Koten, G.; Albrecht, M. *Angew. Chem., Int. Ed.* **2001**, *40*, 3750.
- (5) Singleton, J. T. *Tetrahedron* **2003**, *59*, 1837.
- (6) Milstein, D.; van der Boom, M. E. *Chem. Rev.* **2003**, *103*, 1759.
- (7) Brookhart, M.; Gottker-Schnetmann, I.; White, P. S. *Organometallics* **2004**, *23*, 1766.
- (8) Jensen, C. M.; Wang, Z. H.; Eberhard, M. R.; Matsukawa, S.; Yamamoto, Y. *J. Organomet. Chem.* **2003**, *681*, 189.
- (9) Vicente, J.; Arcas, A.; Galvez-Lopez, M. D.; Jones, P. G. *Organometallics* **2004**, *23*, 3521.
- (10) Sole, D.; Vallverdu, L.; Solans, X.; Font-Bardia, M. *Chem. Commun.* **2005**, 2738.
- (11) Haenel, M. W.; Oevers, S.; Angermund, K.; Kaska, W. C.; Fan, H. J.; Hall, M. B. *Angew. Chem., Int. Ed.* **2001**, *40*, 3596.
- (12) van Koten, G.; Farrington, E. J.; Viviente, E. M.; Williams, B. S.; Brown, J. M. *Chem. Commun.* **2002**, 308.
- (13) Koridze, A. A.; Kuklin, S. A.; Sheloumov, A. M.; Dolgushin, F. M.; Lagunova, V. Y.; Petukhova, I.; Ezernitskaya, M. G.; Peregudov, A. S.; Petrovskii, P. V.; Vorontsov, E. V.; Baya, M.; Poli, R. *Organometallics* **2004**, *23*, 4585.
- (14) Bedford, R. B. *Chem. Commun.* **2003**, 1787.

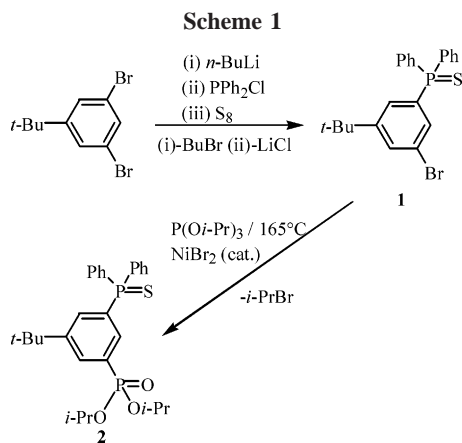
Chart 1



compounds.¹⁷ Among the pincer-type ligands reported so far there are only a few representatives containing different donor sites L and L' in one molecule (types **G**,¹⁸ **H**,¹⁹ **L**¹⁰).

For some time we have been interested in phosphorus-containing O,C,O- and S,C,S-coordinating pincer-type ligands

- (15) Beletskaya, I. P.; Cheprakov, A. V. *J. Organomet. Chem.* **2004**, *689*, 4055.
- (16) Szabo, K. J.; Sebelius, S.; Olsson, V. J. *J. Am. Chem. Soc.* **2005**, *127*, 10478.
- (17) Jensen, C. M. *Chem. Commun.* **1999**, 2443.



of types **P**^{20,21} and **Q**²² respectively (Chart 1). These ligands have been applied in the synthesis of intramolecularly coordinated main group metal and metalloid compounds as well as of palladium complexes. Notably, a related S,C,S-coordinating ligand of type **O**²³ (Chart 1) was reported in 2003.

In continuation of our studies we report here the synthesis of the first O,C,S-coordinating pincer-type ligand of type **R** (Chart 1), in its protonated form, and its triphenyltin derivative. The latter was converted into an intramolecularly coordinated triorganotin cation which showed remarkable stability against moisture but reacted with bromide ion to give, in situ, an intramolecularly P=S-coordinated benzoxaphosphastannole.

Results and Discussion

The one-pot subsequent reaction of 1,3-di-bromo-5-*tert*-butylbenzene with *n*-butyllithium, chlorodiphenylphosphine, and elemental sulfur provided the bromo-substituted triarylphosphane sulfide (3-Br-5-*t*-Bu-C₆H₃)P(S)Ph₂ (**1**) in good overall yield (Scheme 1). Compound **1** is a colorless solid, the molecular structure of which is shown in Figure 1. Selected geometric parameters are collected in Table 1. The phosphorus atom exhibits a distorted tetrahedral configuration (bond angles between 105.0(1)° (C21–P1–C2) and 113.24(8)° (C11–P1–S1). Notably, there are intramolecular S(1)⋯H(1) and S(1)⋯H(12) distances of 2.90(2) and 2.84(2) Å, respectively, being shorter than the sum of the van der Waals radii²⁴ of these atoms (H: 1.20–1.40 Å, S: 1.80 Å). For the parent triphenylphosphine sulfide, Ph₃PS, there is one intramolecular S⋯H distance of 2.79 Å.²⁵

A TAVS reaction²⁶ catalyzed by NiBr₂ of the bromo-substituted triarylphosphane sulfide **1** with tri-isopropyl phosphite, (*i*-PrO)₃P, gave the arylphosphonic acid diisopropyl ester {3-*t*-Bu-5-[P(S)Ph₂]-C₆H₃}P(O)(O-*i*-Pr)₂ (**2**) in moderate yield (Scheme 1). Notably, the reaction is not prevented by the sulfur atom present in compound **1**. The molecular structure of

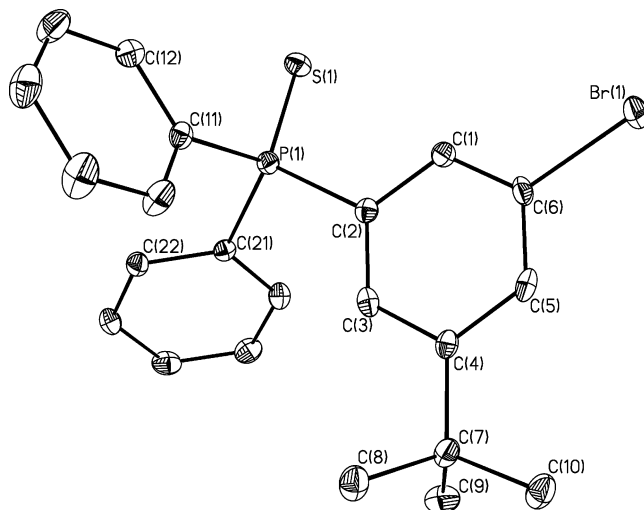


Figure 1. General view (SHELXTL) of a molecule of **1** showing 30% probability displacement ellipsoids and the atom numbering.

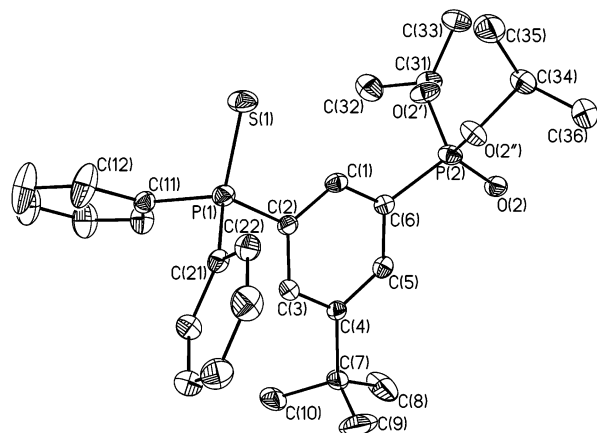


Figure 2. General view (SHELXTL) of a molecule of **2** showing 30% probability displacement ellipsoids and the atom numbering (only one representative of the two symmetry-independent molecules is shown).

Table 1. Selected Bond Lengths (Å) and Bond Angles (deg) for **1** and **2**

	1	2
P(1)–S(1)	1.9556(8)	1.954(1)
P(2)–O(2)		1.461(2)
P(2)–O(2')		1.567(2)
P(2)–O(2'')		1.582(2)
C(2)–P(1)–S(1)	112.73(7)	112.25(9)
C(11)–P(1)–S(1)	113.24(8)	113.49(9)
C(11)–P(1)–C(2)	106.21(9)	106.8(1)
C(11)–P(1)–C(21)	106.2(1)	105.1(1)
C(21)–P(1)–S(1)	112.73(7)	112.73(9)
C(21)–P(1)–C(2)	105.0(1)	105.9(1)
O(2)–P(2)–O(2')		113.8(1)
O(2)–P(2)–O(2'')		117.1(1)
O(2')–P(2)–O(2'')		103.0(1)
O(2)–P(2)–C(6)		113.8(1)
O(2')–P(2)–C(6)		109.6(1)
O(2'')–P(2)–C(6)		97.9(1)
C(1)–C(2)–P(1)	118.7(2)	119.4(2)
C(1)–C(6)–P(2)		120.1(2)

compound **2** is shown in Figure 2, and selected geometric parameters are collected in Table 1.

In the unit cell there are two crystallographically independent molecules whose geometric parameters differ marginally, and consequently the structure of only one molecule is briefly

(18) Milstein, D.; Poverenov, E.; Gandelman, M.; Shimon, L. J. W.; Rozenberg, H.; Ben-David, Y. *Organometallics* **2005**, *24*, 1082.

(19) Milstein, D.; Rybtchinski, B.; Oevers, S.; Montag, M.; Vigalok, A.; Rozenberg, H.; Martin, J. M. L. *J. Am. Chem. Soc.* **2001**, *123*, 9064.

(20) Fischer, J. Diploma thesis, Dortmund University, 2003.

(21) Jurkschat, K.; Fischer, J.; Schürmann, M.; Krause, N.; Löhr, S. *Symposium of the Graduiertenkolleg 352, Synthetic, Mechanistic and Reaction-Engineering Aspects of Metal-Containing Catalysts*, November 17, 2005, TU Berlin, Germany, Book of Abstracts, p 17.

(22) Mehring, M.; Schürmann, M.; Jurkschat, K. *Organometallics* **1998**, *17*, 1227.

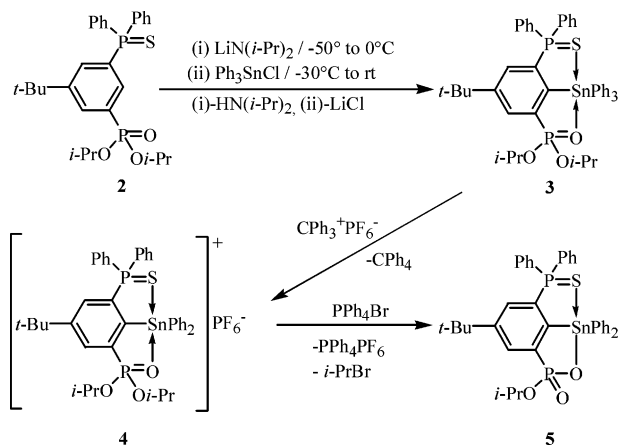
(23) Yamamoto, T.; Kanbara, T. *J. Organomet. Chem.* **2003**, *688*, 15.

(24) Bondi, A. *J. Phys. Chem.* **1964**, *68*, 441.

(25) Ziemer, B.; Rabis, A.; Steinberger, H. U. *Acta Crystallogr. Sect. C: Cryst. Struct. Commun.* **2000**, *56*, E58.

(26) Tavs, P. *Chem. Ber.* **1970**, *103*, 2428.

Scheme 2



discussed. The phosphorus atoms exhibit distorted tetrahedral configurations with the distortion being more pronounced for the phosphonic ester phosphorus (angles between $97.9(1)^\circ$ and $117.1(1)^\circ$ at P2 versus $105.1(1)^\circ$ and $113.49(9)^\circ$ at P1). As in compound **1**, the sulfur atom S(1) points to H(1) with a distance of $2.75(2)$ Å, whereas the O(3) oxygen atom points away, with the consequence of the isopropoxy oxygen atom O(2'') approaching H(1) at a distance of $2.77(2)$ Å. A similar situation was observed for the phosphoryl groups in the related compounds $1,3\text{-}[\text{P}(\text{O})(\text{OR})_2]_2\text{-}5\text{-}t\text{-Bu-C}_6\text{H}_3$ (R = Et, *i*-Pr).^{27,28}

Metalation of compound **2** was achieved with lithium diisopropyl amide, $\text{LiN}(\text{i-Pr})_2$, in diethyl ether/hexane in the temperature range between -50 and 0 °C. Subsequent reaction with triphenyltin chloride, Ph_3SnCl , and recrystallization from dichloromethane/hexane provided the tetraorganotin compound $\{5\text{-}t\text{-Bu-3-}[\text{P}(\text{S})\text{Ph}_2]\text{-2-}(\text{SnPh}_3)\text{-C}_6\text{H}_2\}\text{P}(\text{O})(\text{O-}i\text{-Pr})_2$ (**3**), as its CH_2Cl_2 solvate $\mathbf{3} \cdot 0.6 \text{ CH}_2\text{Cl}_2$, as a colorless crystalline solid in poor yield (Scheme 2). The molecular structure of compound **3** is shown in Figure 3, and selected geometric parameters are collected in Table 2.

As in the related intramolecularly coordinated tetraorganotin compounds $\{4\text{-}t\text{-Bu-2,6-}[\text{P}(\text{O})(\text{OEt})_2]_2\text{C}_6\text{H}_2\}\text{SnPh}_2\text{R}$ (R = Ph,²² Me_3SiCH_2 ²⁹), the tin atom in compound **3** adopts a typical [4+2] coordination. A distorted tetrahedron (mean angle 109.55°) with bond angles ranging between $95.5(1)^\circ$ (C51–Sn1–C61) and $125.5(1)^\circ$ (C1–Sn1–C61) is capped with O(2) at the opposite face of the carbon atom C(61) and with S(1) at the opposite face of the carbon atom C(51), at O(2)⋯Sn(1) and S(1)⋯Sn(1) distances of $2.956(2)$ and $3.513(1)$ Å, respectively. These distances are 0.744 and 0.487 Å shorter than the sums of the van der Waals radii²⁴ of tin (2.20 Å) and oxygen (1.50 Å), and tin and sulfur (1.80 Å), respectively. Notably, these intramolecular O→Sn and S→Sn interactions lengthen the Sn(1)–C(61) and Sn(1)–C(51) distances to $2.161(3)$ and $2.156(3)$ Å, respectively, with respect to the remaining tin–phenyl bond Sn(1)–C(41) ($2.137(3)$ Å). As in the previously reported symmetrically substituted pincer-type ligand-substituted tetraorganotin compound $\{4\text{-}t\text{-Bu-2,6-}[\text{P}(\text{O})(\text{OEt})_2]_2\text{C}_6\text{H}_2\}\text{SnPh}_3$, the C(1)–Sn(1) distance is the longest among the tin–carbon bond lengths and amounts to $2.202(19)$ Å.²² A comparison of the C(1)–C(2)–P(1) ($121.1(3)^\circ$) and C(1)–C(6)–P(2) ($124.5(3)^\circ$) angles, assigned as α , α' angles,²⁷ with the corresponding angles

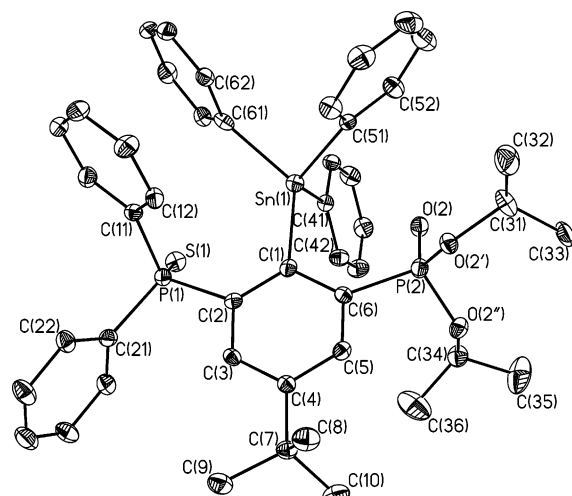


Figure 3. General view (SHELXTL) of a molecule of **3** showing 30% probability displacement ellipsoids and the atom-numbering scheme.

Table 2. Selected Bond Lengths (Å) and Bond Angles (deg) for **3** and **4**

	3	4
Sn(1)–C(1)	2.201(3)	2.159(3)
Sn(1)–C(41)	2.137(3)	2.129(3)
Sn(1)–C(51)	2.156(3)	2.129(3)
Sn(1)–C(61)	2.161(3)	
Sn(1)–O(1)	2.956(2)	2.278(2)
Sn(1)–S(1)	3.513(1)	2.6295(9)
P(1)–S(1)	1.948(1)	2.006(1)
P(2)–O(2)	1.464(2)	1.501(2)
P(2)–O(2')	1.572(2)	1.542(2)
P(2)–O(2'')	1.575(2)	1.562(1)
C(1)–Sn(1)–C(41)	109.7(1)	113.5(1)
C(1)–Sn(1)–C(51)	103.5(1)	122.2(1)
C(1)–Sn(1)–C(61)	125.5(1)	
C(41)–Sn(1)–C(51)	119.1(1)	123.5(1)
C(41)–Sn(1)–C(61)	104.1(1)	
C(51)–Sn(1)–C(61)	95.5(1)	
C(1)–Sn(1)–O(2)	75.7(1)	91.7(1)
C(1)–Sn(1)–S(1)	72.31(9)	98.97(9)
C(41)–Sn(1)–O(2)	70.7(1)	90.1(1)
C(41)–Sn(1)–S(1)	81.42(9)	94.63(9)
C(51)–Sn(1)–O(2)	70.18(9)	79.77(9)
C(51)–Sn(1)–S(1)	158.61(9)	86.12(8)
C(61)–Sn(1)–O(2)	157.7(1)	
C(61)–Sn(1)–S(1)	71.95(9)	
O(2)–Sn(1)–S(1)	126.65(4)	162.42(5)
C(1)–C(2)–P(1)	121.1(3)	119.3(2)
C(1)–C(6)–P(2)	124.5(3)	116.1(2)

in the parent compound **2** ($119.4(2)^\circ$, $120.1(2)^\circ$) suggests, however, that these intramolecular interactions are rather weak. This view is supported by the facts that (i) in comparison with the organotin-free derivative **2** the P(1)–S(1) ($1.948(1)$ Å) and P(2)–O(2) ($1.464(2)$ Å) distances are almost unchanged, (ii) the $\tilde{\nu}(\text{P}=\text{O})$ of 1241 cm^{-1} is rather close to that of compound **2** (1249 cm^{-1}), and (iii) both the O(2) and S(1) atoms are displaced by $0.611(6)$ and $1.497(6)$ Å from the least-squares plane defined by the aromatic carbon atoms C(2)–C(6). In the triorganotin cation **4** (see below) this displacement is much less pronounced (Figure 4).

The weak intramolecular O→Sn and S→Sn interactions in compound **3** are retained in solution. This is especially manifested by its low-frequency ^{119}Sn NMR chemical shift of $\delta -194$ as compared to $\delta -128$ found for tetraphenyltin, SnPh_4 .³⁰

Reaction of the [4+2]-coordinated tetraorganotin compound **3** with triphenylmethyl hexafluorophosphate, $\text{CPh}_3^+\text{PF}_6^-$, pro-

(27) Henn, M.; Jurkschat, K.; Ludwig, R.; Mehring, M.; Peveling, K.; Schürmann, M. *Z. Anorg. Allg. Chem.* **2002**, *628*, 2940–2947.

(28) Henn, M. Ph.D. Thesis, Dortmund University, 2004.

(29) Mehring, M.; Löw, C.; Schürmann, M.; Uhlig, F.; Jurkschat, K.; Mahieu, B. *Organometallics* **2000**, *19*, 4613.

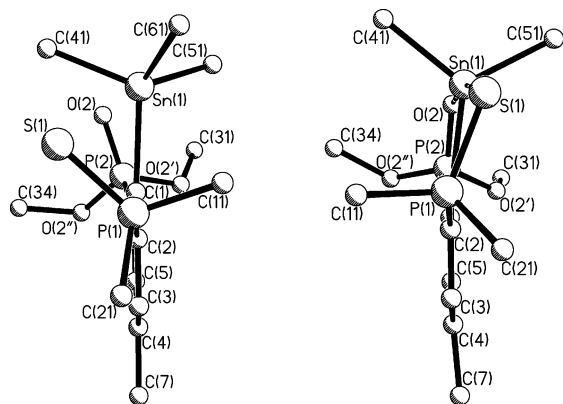


Figure 4. View along the aromatic plane of compounds **3** (left) and **4** (right).

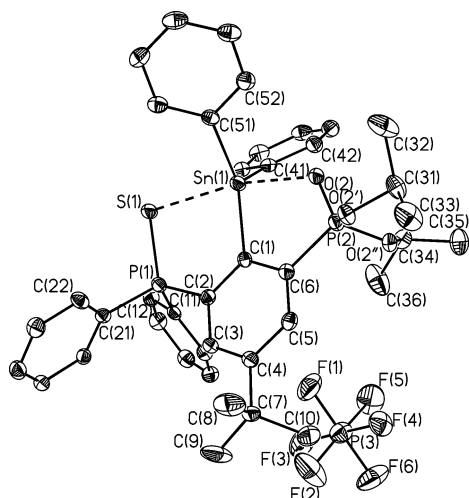


Figure 5. General view (SHELXTL) of an ion pair of **4** showing 30% probability displacement ellipsoids and the atom-numbering scheme.

vided the intramolecularly coordinated triorganotin hexafluorophosphate {4-*t*-Bu-2-[P(O)(O-*i*-Pr)₂]-6-[P(S)Ph₂]-C₆H₂}SnPh₂⁺PF₆⁻ (**4**) as colorless crystals in good yield (Scheme 2). The molecular structure of compound **4** is shown in Figure 5. Selected geometric parameters are given in Table 2.

The tin atom in compound **4** shows a distorted trigonal bipyramidal configuration (geometrical goodness^{31–33} ΔΣ(θ) = 79.44°) with the carbon atoms C(1), C(41), and C(51) in equatorial and the oxygen and sulfur atoms O(2) and S(1), respectively, in axial positions. The Sn(1) atom is deviated by 0.113(2) Å in the direction of S(1) from the plane defined by C(1), C(41), and C(51). Compared with the tetraorganotin derivative **3**, the intramolecular O(2)⋯Sn(1) (2.278(2) Å) and S(1)⋯Sn(1) (2.6295(9) Å) distances are considerably shortened by 0.678 and 0.884 Å, respectively. This shortening causes a simultaneous lengthening of the P(2)–O(2) and P(1)–S(1) distances to 1.501(2) and 2.006(1) Å, respectively, with the former also being illustrated by a decrease of the ν(P=O) to 1155 cm⁻¹. The C(1)–C(2)–P(1) and C(1)–C(6)–P(2) angles (α, α' angles²⁷) decrease to 119.3(2)° and 116.1(2)°, respectively.

The separation between the triorganotin cation {4-*t*-Bu-2-[P(O)(O-*i*-Pr)₂]-6-[P(S)Ph₂]-C₆H₂}SnPh₂⁺ and the hexafluorophosphate anion PF₆⁻ amounts to 5.855(11) Å and indicates no bonding interaction. Overall, the geometrical data including the intramolecular O(2)⋯Sn(1) distance of compound **4** resemble those of the related organotin salt {4-*t*-Bu-2,6-[P(O)(O-*i*-Pr)₂]₂C₆H₂}SnPh₂⁺PF₆⁻³⁴ (geometrical goodness^{31–33} ΔΣ(θ) = 84.6°; O⋯Sn 2.249(2), 2.241(3) Å).

In solution, the triorganotin hexafluorophosphate **4** shows a ¹¹⁹Sn NMR chemical shift of δ -132, which is high-frequency shifted as compared to {4-*t*-Bu-2,6-[P(O)(O-*i*-Pr)₂]₂C₆H₂}SnPh₂⁺PF₆⁻ containing two P=O donor functions (δ -208).³⁴ This difference is in line with the trend observed for the chemical shifts of solutions containing equimolar mixtures of Ph₃SnCl/Ph₃PO (δ -94) and Ph₃SnCl/Ph₃PS (δ -46), respectively.

Another interesting fact to be noticed is the dramatic decrease of the *J*(¹¹⁹Sn–³¹P(O)) couplings, as compared to the related tetraorganotin derivatives {4-*t*-Bu-2,6-[P(O)(O-*i*-Pr)₂]₂C₆H₂}SnPh₃ (35 Hz)³⁴ and **3** (28 Hz), respectively, for both {4-*t*-Bu-2,6-[P(O)(O-*i*-Pr)₂]₂C₆H₂}SnPh₂⁺PF₆⁻³⁴ (5 Hz) and compound **4** to the extent that in the latter this coupling was detected neither in the ¹¹⁹Sn nor in the ³¹P NMR spectrum because of line broadening (ν_{1/2} 9 Hz, 5 Hz). The *J*(¹¹⁹Sn–³¹P(S)) coupling in **4** (37 Hz) decreases as well with respect to compound **3** (56 Hz). The coupling constants actually observed are absolute values and composed of different coupling pathways ²*J*(¹¹⁹Sn–X–³¹P) (X = O, S) and ³*J*(¹¹⁹Sn–C–C–³¹P). These coupling pathways might have different signs and magnitudes, which in turn can change upon changes of the substituent pattern at the tin or phosphorus atoms and/or the conformation of the molecule. The conversion of the tetraorganotin compound **3** to the corresponding triorganotin cation **4** is associated with such a change, and consequently, the magnitude of the coupling constant changes. Similar observations for *o*-Ph₂P(O)C₆H₄-SnMe₂X (X = Me, Br) were already noticed by Weichmann and Schmoll.³⁵

The natural bond orbital (NBO) analyses on model compounds (Table 3) in which the isopropoxy substituents are replaced by ethoxy substituents shows (i) that the positive charge at the tin atom in [R'SnPh₂]⁺ (R' = S, C, O-coordinating ligand; the ethoxy-substituted analogue of the cation in compound **4**) is reduced with respect to [R'SnPh₂]⁺³⁴ (R = O, C, O-coordinating ligand), (ii) that in [R'SnPh₂]⁺ the positive charge at both phosphorus atoms increases with respect to R'H with the effect being more pronounced for the P=O phosphorus atom, and (iii) that in [R'SnPh₂]⁺ the P=O→Sn charge transfer is higher than in [R'SnPh₂]⁺ and slightly dominates over the one induced by P=S→Sn. The results suggest that compared with {4-*t*-Bu-2,6-[P(O)(O-*i*-Pr)₂]₂C₆H₂}SnPh₂⁺ for compound **4** the importance of the canonical formula (II) with the positive charge located at the P=O phosphorus atom increases, without, however, dominating over canonical formula (I) (Chart 2). Apparently, the charge distribution can be controlled by the identity of the donor atom. These statements get further support by the ν(P=O) being smaller for compound **4** (1155 cm⁻¹) than for {4-*t*-Bu-2,6-[P(O)(O-*i*-Pr)₂]₂C₆H₂}SnPh₂⁺PF₆⁻ (1177 cm⁻¹).³⁴ On the other hand, the Wiberg bond indices^{36,37} of 0.4040 and 0.2157 indicate a higher covalent character of the Sn–S as compared to the Sn–O bond, and consequently, the canonical formula (III) appears also to be meaningful. At this point it

(30) Lycka, A.; Snobl, D.; Handlir, K.; Holecck, J.; Nadvornik, M. *Collect. Czech. Chem. Commun.* **1981**, *46*, 1383.

(31) Kolb, U.; Beuter, M.; Gerner, M.; Dräger, M. *Organometallics* **1994**, *13*, 4413.

(32) Kolb, U.; Beuter, M.; Dräger, M. *Inorg. Chem.* **1994**, *33*, 4522.

(33) Kolb, U.; Dräger, M.; Jousseau, B. *Organometallics* **1991**, *10*, 2737.

(34) Peveling, K.; Henn, M.; Löw, C.; Mehrling, M.; Schürmann, M.; Costisella, B.; Jurkschat, K. *Organometallics* **2004**, *23*, 1501.

(35) Weichmann, H.; Schmoll, C. *Z. Chem.* **1984**, *24*, 390.

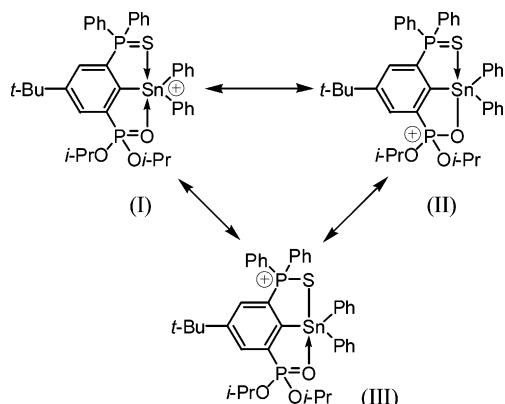
(36) Mayer, I. *Chem. Phys. Lett.* **1983**, *97*, 270.

(37) Wiberg, K. A. *Tetrahedron* **1968**, *24*, 1083.

Table 3. Selected Results of the NBO Analysis for 5-*t*-Bu-1,3-[P(O)(OEt)₂]₂C₆H₃ (RH), {4-*t*-Bu-2,6-[P(O)(OEt)₂]₂-C₆H₂}SnPh₂⁺ (R₂SnPh₂⁺), {3-*t*-Bu-5-[P(S)Ph₂]-C₆H₃}P(O)(OEt)₂ (R'H), and {4-*t*-Bu-2-[P(O)(OEt)₂]-6-[P(S)Ph₂]-C₆H₂}SnPh₂⁺ (R'SnPh₂⁺) Calculated at the B3LYP/LANL2DZ Level of Theory (atomic charges; charge transfer, au; orbital occupation)

	NBO charges				M	charge transfer		occ(p(M))
	P=O	P=S	P=O	P=S		P=O→M	P=S→M	
RH	+2.282		-1.053					
R'H	+2.274	+1.231	-1.046	-0.592				
R ₂ SnPh ₂ ⁺	+2.355		-1.158		+2.350	0.122		0.198
R'SnPh ₂ ⁺	+2.361		-1.159					
R'SnPh ₂ ⁺	+2.363	+1.297	-1.164	-0.548	+2.165	0.135	0.115	0.284

Chart 2



should be mentioned that the classification of so-called *dative* bonds as being covalent or ionic is still a matter of controversial debate.³⁸

The triorganotin hexafluorophosphate **4** is stable toward moisture, but it does react with tetraphenylphosphonium bromide, Ph₄PBr (Scheme 2), in a manner analogous to that for {4-*t*-Bu-2,6-[P(O)(OEt)₂]₂C₆H₂}SnPh₂⁺PF₆⁻.³⁴ Thus, the ³¹P NMR spectrum of a C₂D₂Cl₄ solution containing equimolar amounts of compound **4** and Ph₄PBr, which had been heated to 65° C for 6 h, exhibited two equally intense doublet resonances at δ 15.2 (ν_{1/2} 1.6 Hz, J(³¹P–³¹P) = 2.0 Hz) and δ 51.4 (ν_{1/2} 4 Hz, J(³¹P–³¹P) = 2.0 Hz, J(³¹P–¹¹⁹Sn) = 64.8 Hz). The ¹¹⁹Sn NMR spectrum of the same solution contained a resonance at δ -168 (ν_{1/2} 18 Hz, J(³¹P–¹¹⁹Sn) = 65 Hz). The signals are assigned to hypercoordinated benzoxaphosphastannole derivative **5** (Scheme 2), which, however, was not isolated from the reaction mixture. In both the ³¹P and ¹¹⁹Sn NMR spectra, again only one instead of the expected two J(³¹P–¹¹⁹Sn) couplings were observed. The explanation for this is the same as given above. The assignment of the NMR signals gets support from the electrospray mass spectrum (positive mode) of the crude product, showing a mass cluster centered at *m/z* = 745.1 and which corresponds to the empirical formula C₃₇H₃₉O₃P₂SSn, i.e., protonated benzoxaphosphastannole [**5**-H]⁺.

Conclusion

In this report we have added a novel representative to the family of pincer-type ligands, namely, in its protonated form, the unsymmetrically O,C,S-coordinating ligand {3-*t*-Bu-5-[P(S)Ph₂]-C₆H₃}P(O)(O-*i*-Pr)₂ combining both the hard and soft donor atoms oxygen and sulfur, respectively. The utility of this ligand for the synthesis of the intramolecularly coordinated triorganostannyl cation salt {4-*t*-Bu-2-[P(O)(O-*i*-Pr)₂]-6-[P(S)Ph₂]-C₆H₂}SnPh₂⁺PF₆⁻ (**4**) has been demonstrated, and, by MO calculations, the possibility to control the positive charge and

its distribution in the cation by the identity of the coordinating donor atoms has been shown. This work contributes to the general understanding of structure and reactivity of organoelement-14 cations as a field of ongoing interest.^{39–45} Given the fact that organotin-based Lewis acids^{46,47} are catalysts for a variety of organic reactions, it even suggests the possibility for tailoring such catalysts by variation of coordinating donor atoms.

Experimental Section

General Considerations. All solvents were dried and purified by standard procedures. All reactions were carried out under an atmosphere of dry argon. SnPh₃Cl and CPh₃⁺PF₆⁻ were purchased from Lancaster and Aldrich, respectively, and used without further purification. IR spectra (cm⁻¹) were recorded on a Bruker IFS 28 spectrometer. Varian Mercury 200, Bruker DPX-300, and DRX-400 spectrometers were used to obtain ¹H, ¹³C, ³¹P, and ¹¹⁹Sn NMR spectra. ¹H, ¹³C, ³¹P, and ¹¹⁹Sn NMR chemical shifts are given in ppm and were referenced to Me₄Si, H₃PO₄ (85%, ³¹P) and Me₄Sn (¹¹⁹Sn). NMR spectra were recorded at room temperature unless otherwise stated. The atom numberings given in Figures 3 and 4 apply for the assignment of the ¹³C resonances of compounds **3** and **4**. Elemental analyses were performed on a LECO-CHNS-932 analyzer.

Electrospray mass spectra were recorded in the positive mode on a Thermoquest-Finnigan instrument using CH₃CN as the mobile phase. The samples were introduced as solution in a mixture of CH₃CN and 1% formic acid (9:1 ratio) (*c* = 10⁻⁴ mol L⁻¹) via a syringe pump operating at 0.5 μL/min. The capillary voltage was 4.5 kV, while the cone skimmer voltage was varied between 50 and 250 kV. Identification of the inspected ions was assisted by comparison of experimental and calculated isotope distribution patterns. The *m/z* values reported correspond to those of the most intense peak in the corresponding isotope pattern.

Molecular Orbital Calculations. Calculations of the structures and energies of 5-*t*-Bu-1,3-[P(O)(OEt)₂]₂C₆H₃,³⁴ {4-*t*-Bu-2,6-[P(O)(OEt)₂]₂-C₆H₂}SnPh₂⁺,³⁴ {3-*t*-Bu-5-[P(S)Ph₂]-C₆H₃}P(O)(OEt)₂, and {4-*t*-Bu-2-[P(O)(OEt)₂]-6-[P(S)Ph₂]-C₆H₂}SnPh₂⁺ have been carried out at the density functional (B3LYP) level with the Gaussian 98 program⁴⁸ using the internal stored LANL2DZ basis set. This basis

(39) Zharov, I.; Michl, J. *The Chemistry of Organic Germanium, Tin, and Lead Compounds*; Rappoport, Z., Ed.; Wiley & Sons: New York, 2002; Vol. 2, pp 633–652.

(40) Müller, T. *Adv. Organomet. Chem.* **2005**, *53*, 155.

(41) Kašná, B.; Jambor, R.; Dostál, L.; Císarová, I.; Holeček, J. *J. Organomet. Chem.* **2006**, *691*, 1554.

(42) Choi, N.; Lickiss, P. D.; McPartlin, M.; Masangane, P. C.; Veneziani, G. L. *Chem. Commun.* **2005**, 6023.

(43) Kost, D.; Kalikhman, I. *Adv. Organomet. Chem.* **2004**, *50*, 1.

(44) Beckmann, J.; Dakternieks, D.; Duthie, A.; Mitchell, C. *Organometallics* **2004**, *23*, 6150.

(45) Kašná, B.; Jambor, R.; Dostál, L.; Kolárová, L.; Císarová, I.; Holeček, J. *Organometallics* **2006**, *25*, 5300.

(46) Ishihara, K. Sn(II) and Sn(IV) Lewis Acids. In *Lewis Acids in Organic Synthesis*; Yamamoto, H., Ed.; Wiley-VCH: Weinheim, 2000; p 395.

(47) Durand, S.; Sakamoto, K.; Fukuyama, T.; Orita, A.; Otera, J.; Duthie, A.; Dakternieks, D.; Schulte, M.; Jurkschat, K. *Organometallics* **2000**, *19*, 3220.

(38) Kocher, N.; Henn, J.; Gostevskii, B.; Kost, D.; Kalikhman, I.; Engels, B.; Stalke, D. *J. Am. Chem. Soc.* **2004**, *126*, 5563.

Table 4. Crystallographic Data for 1–4

	1	2	3	4
formula	C ₂₂ H ₂₂ BrPS	C ₂₈ H ₃₆ O ₃ P ₂ S	C ₄₆ H ₅₀ O ₃ P ₂ SSn·0.6CH ₂ Cl ₂	[C ₄₀ H ₄₅ O ₃ P ₂ SSn] ⁺ [PF ₆] ⁻
fw	429.34	514.57	914.51	931.42
cryst syst	monoclinic	triclinic	triclinic	triclinic
cryst size, mm	0.25 × 0.25 × 0.23	0.20 × 0.20 × 0.18	0.30 × 0.25 × 0.25	0.10 × 0.05 × 0.05
space group	P2 ₁ /c	P $\bar{1}$	P $\bar{1}$	P $\bar{1}$
a, Å	8.9777(2)	11.2637(10)	12.3286(9)	11.1588(5)
b, Å	9.3145(2)	14.920(2)	13.3439(8)	11.8227(11)
c, Å	24.3328(6)	17.289(2)	15.2367(8)	16.2506(14)
α, deg	90	84.923(4)	113.043(3)	88.244(3)
β, deg	93.1687(12)	89.342(7)	92.551(4)	74.999(5)
γ, deg	90	77.652(7)	104.670(3)	86.297(5)
V, Å ³	2031.67(8)	2827.1(6)	2202.2(2)	2066.3(2)
Z	4	4	2	2
ρ _{calcd} , Mg/m ³	1.404	1.209	1.379	1.497
μ, mm ⁻¹	2.207	0.254	0.812	0.849
F(000)	880	1096	942	948
θ range, deg	3.15 to 27.48	2.95 to 25.35	2.94 to 27.49	3.03 to 26.37
index ranges	-11 ≤ h ≤ 11 -12 ≤ k ≤ 12 31 ≤ l ≤ 31	-13 ≤ h ≤ 13 -17 ≤ k ≤ 17 -20 ≤ l ≤ 20	-15 ≤ h ≤ 15 -17 ≤ k ≤ 16 -19 ≤ l ≤ 19	-13 ≤ h ≤ 13 -14 ≤ k ≤ 14 -19 ≤ l ≤ 20
no. of reflns colld	19 432	33 673	29 671	30 785
completeness to θ _{max} , %	99.7	99.5	99.6	99.3
no. of indep reflns/R _{int}	4641/0.043	10291/0.034	9851/0.057	8399/0.05
no. of reflns obsd with I > 2σ(I)	2762	4815	4851	4501
no. of refined params	268	727	519	487
GOF (F ²)	0.864	0.775	0.775	0.721
R1 (F) (I > 2σ(I))	0.0317	0.0422	0.0455	0.0390
wR2 (F ²) (all data)	0.0592	0.0859	0.0766	0.0610
(Δ/σ) _{max}	0.001	< 0.001	< 0.001	0.001
largest diff peak/hole, e/Å ³	0.409/-0.441	0.465/-0.303	1.216/-0.634	0.851/-0.466

set was previously shown to be appropriate for large organotin compounds including intra- and intermolecular coordination.^{34,49–53}

In combination with an NBO analysis it provides a qualitative picture of the bonding situation, although the geometry optimization of the P=O and P=S bond lengths is inaccurate. Comparing the results obtained by single-crystal X-ray structure analyses with those obtained by calculations, systematic errors of about 6% and 8% are observed for the P=O³⁴ and P=S bond lengths, respectively. For the calculations shown in Table 4 the O-*i*-Pr groups of compound **4** were replaced by OEt groups in order to compare the results with those recently reported.³⁴ However, the results obtained for {4-*t*-Bu-2-[P(O)(O-*i*-Pr)₂]-6-[P(S)Ph₂]-C₆H₅}SnPh₂⁺ do not show any significant difference. Having these results in mind and being forced to use the same level of theory for all compounds to get comparable results, the LANL2DZ basis set was chosen. Additionally, the wave functions were analyzed by the natural bond orbital (NBO) method,^{54,55} a standard option of Gaussian 98. The NBO analysis explains the strength of coordinative bonds in terms of donor–acceptor interactions between doubly occupied lone pair

orbitals and unoccupied antibonding orbitals and provides atomic charges that are more reliable than Mulliken charges.

Crystallography. Intensity data for the colorless crystals were collected on a Nonius KappaCCD diffractometer with graphite-monochromated Mo Kα (0.71073 Å) radiation at 173(1) K. The data collection covered almost the whole sphere of reciprocal space with three (**1**, **4**) and four (**2**, **3**) sets at different *k*-angles with 302 (**1**), 210 (**2**), 540 (**3**), and 237 (**4**) frames via ω-rotation (Δ/ω = 1°) (**1**, **3**, **4**) and (Δ/ω = 2°) (**2**) at two times 10 s (**3**, **4**), 12.5 s (**2**), and 60 s (**4**) per frame. The crystal-to-detector distances were 3.4 cm (**1**, **2**, **4**) and 4.0 cm (**3**). Crystal decays were monitored by repeating the initial frames at the end of data collection. The data were not corrected for absorption effects. Analyzing the duplicate reflections there were no indications for any decay. The structure was solved by direct methods using SHELXS97⁵⁶ and successive difference Fourier syntheses. Refinement applied full-matrix least-squares methods with SHELXL97.⁵⁷

The H atoms were placed in geometrically calculated positions using a riding model with isotropic temperature factors constrained at 1.2 for non-methyl and at 1.5 for methyl groups times *U*_{eq} of the carrier C atom. In **1** and **2** the coordinates (ref._{x,y,z}) of the aryl hydrogen atoms were refined.

In **2** and **3** isopropoxy groups are disordered over two positions with occupancies of 0.5 (O(4''), C(73), C(74), C(75), O(4'''), C(73'), C(74'), C(75')) (**2**) and 0.4 (C(33'')) and 0.6 (C(33) (**3**)). Each chlorine atom (Cl(1), Cl(2), Cl(1'), Cl(2'), Cl(3), Cl(4), Cl(3'), Cl(4')) of the solvent molecules CH₂Cl₂ in **3** is disordered over two positions and was isotropically refined with occupancies of 0.15, whereas the carbon atoms (C(71), C(81)) were isotropically refined with occupancies of 0.3.

Atomic scattering factors for neutral atoms and real and imaginary dispersion terms were taken from International Tables for X-ray Crystallography.⁵⁸ The figures were created by SHELXTL.⁵⁹ Crystallographic data are given in Table 4; selected bond distances and angles, in Table 1 (**1**, **2**) and Table 2 (**3**, **4**).

(48) Frisch, M. J.; Trucks, G. W.; Schlegel, H. B.; Scuseria, G. E.; Robb, M. A.; Cheeseman, J. R.; Zakrzewski, V. G.; Montgomery, J. A.; Stratmann, R. E.; Burant, J. C.; Dapprich, S.; Millian, J. M.; Daniels, A. D.; Kudin, K. N.; Strain, M. C.; Farkas, O.; Tomasi, J.; Barone, V.; Cossi, M.; Cammi, R.; Mennucci, B.; Pomelli, C.; Adamo, C.; Clifford, S.; Ochterski, J.; Petersson, G. A.; Ayala, P. Y.; Cui, Q.; Morokuma, K.; Malick, D. K.; Rabuck, A. D.; Raghavachari, K.; Foresman, J. B.; Cioslowski, J.; Ortiz, J. V.; Stefanov, B. B.; Liu, G.; Liashenko, A.; Piskorz, P.; Komaromi, I.; Bomperts, R.; Martin, R. L.; Fox, D. J.; Keith, T.; Al-Laham, M. A.; Peng, C. Y.; Nanayakkara, A.; Gonzalez, C.; Challacombe, M.; Gill, P. M. W.; Johnson, B. G.; Chen, W.; Wong, M. W.; Andres, J. L.; Head-Gordon, M.; Replogle, E. S.; Pople, J. A. *Gaussian 98*; Gaussian Inc.: Pittsburgh, 1998.

(49) Buntine, M. A.; Hall, V. J.; Kosovel, F. J.; Tiekink, E. R. T. *J. Phys. Chem. A* **1998**, *102*, 2472.

(50) Obora, Y.; Nakanishi, M.; Tokunaga, M.; Tsuji, Y. *J. Org. Chem.* **2002**, *67*, 5835.

(51) Ryner, M.; Finne, A.; Albertsson, A.-C.; Kricheldorf, H. R. *Macromolecules* **2001**, *34*, 7281.

(52) Hu, Y.-H.; Su, M.-D. *J. Phys. Chem. A* **2003**, *107*, 4130.

(53) Tani, K.; Kato, S.; Kanda, T.; Inagaki, S. *Org. Lett.* **2001**, *3*, 655.

(54) Reed, A. E.; Curtiss, L. A.; Weinhold, F. *Chem. Rev.* **1988**, *88*, 899.

(55) King, B. F.; Weinhold, F. *J. Phys. Chem.* **1995**, *103*, 333.

(56) Sheldrick, G. M. *Acta Crystallogr. A* **1990**, *46*.

(57) Sheldrick, G. M. *SHELXL97*; University of Göttingen, 1997.

(58) *International Tables for X-ray Crystallography*; Kluwer Academic Publishers: Dordrecht, 1992; Vol. C.

(3-Bromo-5-*tert*-butylphenyl)diphenylphosphane Sulfide, (3-Br-5-*t*-Bu-C₆H₃)P(S)Ph₂ (1). 1,3-Dibromo-5-*tert*-butylbenzene (28.3 g, 98.6 mmol) was dissolved in dry diethyl ether. Under magnetic stirring at $-70\text{ }^{\circ}\text{C}$, a solution of *n*-BuLi in *n*-hexane (63.1 mL, 1.6 M) was added dropwise within 3 h. Progress of the metal-halide exchange was controlled by GC/MS. The reaction mixture was kept at $-70\text{ }^{\circ}\text{C}$, and chlorodiphenylphosphane (18.8 mL, 101.5 mmol) was added dropwise within 45 min. The reaction was warmed to $0\text{ }^{\circ}\text{C}$, and sulfur (3.3 g, 103.5 mmol) was added in small portions. After the reaction mixture had been stirred overnight, the precipitate was filtered and subsequently washed with water, in order to remove the lithium salts, and diethyl ether. Subsequent recrystallization with diethyl ether gave 24.5 g (58%) of **1** as a colorless solid; mp $131\text{ }^{\circ}\text{C}$. Single crystals suitable for X-ray diffraction analysis were grown by slow evaporation of a hexane/diethyl ether solution.

¹H NMR (400.13 MHz, CDCl₃): δ 1.23 (s, 9H), 7.44 (m, 4H), 7.51 (m, 2H), 7.56 (ddd, ³*J*(¹H-³¹P) = 12.8 Hz, ⁴*J*(¹H-¹H) = 1.5 Hz, 1.5 Hz, 1H), 7.62 (d, ⁴*J*(¹H-¹H) = 1.5 Hz, 1H), 7.72-7.65 (complex pattern, 5H). ¹³C{¹H} NMR (100.63 MHz, CDCl₃): δ 30.8 (C(CH₃)₃), 35.0 (C(CH₃)₃), 122.7 (d, ³*J*(¹³C-³¹P) = 16.5 Hz, C₃-Br), 128.0 (d, ²*J*(¹³C-³¹P) = 11.2 Hz, C_{2,6}), 128.4 (d, ³*J*(¹³C-³¹P) = 12.6 Hz, C_{Ph}), 131.6 (d, ⁴*J*(¹³C-³¹P) = 3.4 Hz, C_{Ph}), 131.6 (d, ²*J*(¹³C-³¹P) = 12.1 Hz, C_{2,6}), 131.7 (d, ⁴*J*(¹³C-³¹P) = 2.4 Hz, C₄), 132.0 (d, ²*J*(¹³C-³¹P) = 10.7 Hz, C_{Ph}), 132.3 (d, ¹*J*(¹³C-³¹P) = 85.0 Hz, C_{Ph}), 135.0 (d, ¹*J*(¹³C-³¹P) = 82.1 Hz, C₁), 153.7 (d, ³*J*(¹³C-³¹P) = 11.7 Hz, C₅-C(CH₃)₃). ³¹P{¹H} NMR (121.49 MHz, D₂O): δ 44.1. Anal. Calcd for C₂₂H₂₂BrPS: C, 61.5; H, 5.2. Found: C, 61.1; H, 5.3.

[3-*tert*-Butyl-5-(diphenylphosphinothioyl)phenyl]phosphonic Acid Di-isopropyl Ester, {3-*t*-Bu-5-[P(S)Ph₂]-C₆H₃}P(O)(O-*i*-Pr)₂ (2). (3-Bromo-5-*tert*-butylphenyl)diphenylphosphane sulfide (**1**) (9.59 g, 22.3 mmol) and nickel bromide (0.49 g, 2.23 mmol) were heated at $165\text{ }^{\circ}\text{C}$. Phosphoric acid tri-isopropyl ester (6.1 mL, 24.5 mmol) was added dropwise within 30 min and the reaction mixture was kept at $165\text{ }^{\circ}\text{C}$ for another 30 min, during which it turned black. The crude product was purified by column chromatography (silica, diethyl ether) to give 6.8 g (59%) of compound **2** as a colorless oil, which solidified after it had been kept overnight at $0\text{ }^{\circ}\text{C}$. Single crystals (mp $86\text{ }^{\circ}\text{C}$) suitable for X-ray diffraction analysis were grown by slow evaporation of a hexane/dichloromethane solution.

¹H NMR (400.13 MHz, CDCl₃): δ 1.12 (d, ³*J*(¹H-¹H) = 6.3 Hz, 6H; CH(CH₃)₂), 1.28 (d, ³*J*(¹H-¹H) = 6.3 Hz, 6H; CH(CH₃)₂), 1.28 (s, 9H; C(CH₃)₃), 4.61 (d, septet, ³*J*(¹H-¹H) = ³*J*(¹H-³¹P) = 6.3 Hz, 2H; CH(CH₃)₂), 7.43 (m, 4H; H_{Ph}), 7.50 (m, 2H; H_{Ph-para}), 7.64-7.75 (complex pattern, 5H; H_{Ph} and H₆), 7.95 (d, ³*J*(¹H-³¹P) = 14.0 Hz, 1H; H_{2,4}), 8.04 (d, ³*J*(¹H-³¹P) = 14.6 Hz, 1H; H_{2,4}). ¹³C{¹H} NMR (100.63 MHz, CDCl₃): δ 23.5 (d, ³*J*(¹³C-³¹P) = 4.9 Hz; CH(CH₃)₂), 23.8 (d, ³*J*(¹³C-³¹P) = 3.9 Hz; CH(CH₃)₂), 30.9 (s, C(CH₃)₃), 35.1 (s, C(CH₃)₃), 70.8 (d, ²*J*(¹³C-³¹P) = 5.8 Hz; CH(CH₃)₂), 128.4 (d, ³*J*(¹³C-³¹P) = 12.6 Hz; C_{Ph}), 130.4 (dd, ¹*J*(¹³C-³¹P) = 188.0 Hz, ³*J*(¹³C-³¹P) = 11.7 Hz; C₁-P), 131.5 (d, ⁴*J*(¹³C-³¹P) = 2.9 Hz; C_{Ph-para}), 131.9 (dd, ²*J*(¹³C-³¹P) = 10.7 Hz, ⁴*J*(¹³C-³¹P) = 2.9 Hz; C_{2,4}), 132.2 (dd, ²*J*(¹³C-³¹P) = 10.7 Hz, 10.7 Hz; C₆), 132.2 (d, ²*J*(¹³C-³¹P) = 10.7 Hz; C_{Ph}), 133.1 (dd, ²*J*(¹³C-³¹P) = 11.7 Hz, ⁴*J*(¹³C-³¹P) = 2.9 Hz; C_{2,4}), 133.3 (dd, ¹*J*(¹³C-³¹P) = 85.6 Hz, ³*J*(¹³C-³¹P) = 14.5 Hz; C₅-P), 151.7 (dd, ³*J*(¹³C-³¹P) = 13.6 Hz, 11.2 Hz; C₃-C(CH₃)₃). ³¹P{¹H} NMR (81.01 MHz, CDCl₃): δ 16.3 (d, *J*(³¹P-³¹P) = 5.9 Hz; P=O), 44.6 (d, *J*(³¹P-³¹P) = 5.9 Hz; P=S). IR (KBr): $\tilde{\nu}$ (P=O) 1249 cm⁻¹. Anal. Calcd for C₂₈H₃₆O₃P₂S: C, 65.4; H, 7.1. Found: C, 65.1; H, 6.9.

[5-*tert*-Butyl-3-(diphenylphosphinothioyl)-2-(triphenylstannyl)phenyl]phosphonic Acid Di-isopropyl Ester, {5-*t*-Bu-3-[P(S)Ph₂]-2-(SnPh₃)-C₆H₂}P(O)(O-*i*-Pr)₂ (3). A solution of *i*-Pr₂NLi (6.8 mL,

0.49 M, 3.46 mmol) in diethyl ether/hexane (2:1) was added dropwise at $-50\text{ }^{\circ}\text{C}$ and under magnetic stirring to a solution of the arylphosphonic acid diisopropyl ester {3-*t*-Bu-5-[P(S)Ph₂]-C₆H₃}P(O)(O-*i*-Pr)₂ (**2**) (1.48 g, 2.88 mmol) in diethyl ether (35 mL). The reaction mixture was allowed to warm to $0\text{ }^{\circ}\text{C}$ and was stirred at this temperature for 9 h. Then the reaction mixture was cooled to $-20\text{ }^{\circ}\text{C}$ and triphenyltin chloride (1.33 g, 3.46 mmol) was added in one portion. The suspension was stirred overnight while reaching room temperature. The solvent was removed in vacuo. Dichloromethane and a saturated aqueous KF solution were added to the residue, and the resulting mixture was stirred for 10 min. The precipitate formed at the interlayer was filtered, and the organic phase was separated, washed again with aqueous KF solution, and dried over MgSO₄ followed by filtration. The solvent of the filtrate was evaporated in vacuo, and the residue was purified by column chromatography (silica, diethyl ether) to give starting material **2** (0.97 g, 1.88 mmol) and a product-containing fraction. The latter was purified by crystallization from a hexane/dichloromethane mixture to give compound **3** (0.24 g, 10%), as its dichloromethane solvate **3**·CH₂Cl₂, as colorless crystals with a mp of $114\text{ }^{\circ}\text{C}$.

¹H NMR (400.13 MHz, CD₂Cl₂): δ 0.83 (d, ³*J*(¹H-¹H) = 6.3 Hz, 6H; CH(CH₃)₂), 1.12 (d, ³*J*(¹H-¹H) = 6.3 Hz, 6H; CH(CH₃)₂), 1.13 (s, 9H; C(CH₃)₃), 3.94 (d of septet, 2H, ³*J*(¹H-¹H) = ³*J*(¹H-³¹P) = 6.3 Hz, 2H; CH(CH₃)₂), 5.27 (s, 2H, CH₂Cl₂), 7.01-7.10 (9H, unresolved), 7.60-7.78 (17H, unresolved), 7.85 (d, ³*J*(¹H-³¹P) = 13.3 Hz, 1H; C_{3,5}). ¹³C{¹H} NMR (100.63 MHz, CDCl₃): δ 23.4 (d, ³*J*(¹³C-³¹P) = 5.8 Hz; CH(CH₃)₂), 23.9 (d, ³*J*(¹³C-³¹P) = 2.9 Hz; CH(CH₃)₂), 30.6 (s; C(CH₃)₃), 34.4 (s; C(CH₃)₃), 70.3 (d, ²*J*(¹³C-³¹P) = 5.8 Hz; CH(CH₃)₂), 126.6 (s, ⁴*J*(¹³C-¹¹⁹Sn) = 10.6 Hz, Sn-C_{para}), 127.1 (s, ²*J*(¹³C-¹¹⁹Sn) = 54.4 Hz; Sn-C_{ortho}), 128.4 (d, ²*J*(¹³C-³¹P) = 12.6 Hz; P-Ph_{ortho}), 131.0 (d, ⁴*J*(¹³C-³¹P) = 2.9 Hz; P-Ph_{para}), 131.7 (d, ³*J*(¹³C-³¹P) = 10.7 Hz; P-Ph_{meta}), 132.2 (dd, ²*J*(¹³C-³¹P) = 10.7 Hz, ⁴*J*(¹³C-³¹P) = 2.9 Hz; C_{3,5}), 133.2 (d, ¹*J*(¹³C-³¹P) = 83.6 Hz; C_{2,6}), 135.2 (dd, ²*J*(¹³C-³¹P) = 14.8 Hz, ⁴*J*(¹³C-³¹P) = 2.9 Hz; C_{3,5}), 137.1 (s, ³*J*(¹³C-¹¹⁹Sn) = 36.9 Hz; Sn-C_{meta}), 148.1 (s; Sn-C_{ipso}), 149.4 (dd, ³*J*(¹³C-³¹P) = 12.1 Hz, 11.2 Hz; C₄), 153.3 (dd, ²*J*(¹³C-³¹P) = 24.3 Hz, 23.3 Hz; C₁). C₂ and C₆ were not assigned unambiguously. ³¹P{¹H} NMR (81.01 MHz, CDCl₃): δ 18.5 (d, *J*(³¹P-³¹P) = 5.2 Hz, *J*(³¹P-¹¹⁹Sn) = 27.5 Hz); P=O, 50.0 (d, *J*(³¹P-³¹P) = 5.2 Hz, *J*(³¹P-¹¹⁹Sn) = 56.1 Hz); P=S). ¹¹⁹Sn{¹H} NMR (111.92 MHz, CDCl₃): δ -194 (dd, *J*(¹¹⁹Sn-³¹P) = 56 Hz, 28 Hz). IR (KBr): $\tilde{\nu}$ (P=O) 1241 cm⁻¹. Anal. Calcd for C₄₆H₅₀O₃P₂SSn·CH₂Cl₂: C, 59.5; H, 5.5. Found: C, 59.5; H, 5.6.

[4-*tert*-Butyl-2-(di-isopropoxyphosphoryl)-6-(diphenylphosphinothioyl)phenyl]diphenylstannyl Hexafluorophosphate, {4-*t*-Bu-2-[P(O)(O-*i*-Pr)₂]-6-[P(S)Ph₂]-C₆H₂}SnPh₂⁺PF₆⁻ (4). To a solution of **3** (46.0 mg, 0.05 mmol) in C₂D₂Cl₄ (1.5 mL) was added triphenylmethyl hexafluorophosphate (19.4 mg, 0.05 mmol). After the reaction mixture had been stirred at room temperature overnight the solvent was removed in vacuo and the crude product was dissolved in dichloromethane. Slow evaporation of the solvent first gave crystals of tetraphenylmethane. After these crystals had been filtered slow evaporation of the solvent was continued to provide 44 mg (94%) of compound **4** as colorless crystals (mp $160\text{ }^{\circ}\text{C}$) suitable for X-ray diffraction analysis.

¹H NMR (300.13 MHz, CDCl₃): δ 1.11 (d, ³*J*(¹H-¹H) = 6.2 Hz, 6H; CH(CH₃)₂), 1.23 (d, ³*J*(¹H-¹H) = 6.3 Hz, 6H; CH(CH₃)₂), 1.31 (s, 9H; C(CH₃)₃), 4.48 (d, septet, ³*J*(¹H-¹H) = ³*J*(¹H-³¹P) = 6.2 Hz, 2H; CH(CH₃)₂), 7.34-7.44 (6H, unresolved), 7.60-7.78 (14H, unresolved), 7.91 (d, ³*J*(¹H-³¹P) = 11.3 Hz, 1H; H_{3,5}), 8.05 (d, ³*J*(¹H-³¹P) = 13.5 Hz, 1H; H_{3,5}). ¹³C{¹H} NMR (100.63 MHz, CDCl₃): δ 23.5 (d, ³*J*(¹³C-³¹P) = 5.8 Hz; CH(CH₃)₂), 23.6 (d, ³*J*(¹³C-³¹P) = 5.3 Hz; CH(CH₃)₂), 29.7 (d, ³*J*(¹³C-³¹P) = 5.3 Hz; C(CH₃)₃), 30.8 (s; C(CH₃)₃), 36.7 (s; C(CH₃)₃), 75.8 (d, ²*J*(¹³C-³¹P) = 6.3 Hz; CH(CH₃)₂), 126.2 (d, ¹*J*(¹³C-³¹P) = 87.5 Hz;

P-Ph_{ipso}), 129.2 (s, $^2J(^{13}\text{C}-^{119}\text{Sn}) = 76.5$ Hz; Sn-C_{ortho}), 130.0 (d, $^2J(^{13}\text{C}-^{31}\text{P}) = 13.6$ Hz; P-Ph_{ortho}), 130.5 (s, $^4J(^{13}\text{C}-^{119}\text{Sn}) = 15.5$ Hz; Sn-C_{para}), 132.2 (dd, $^2J(^{13}\text{C}-^{31}\text{P}) = 12.6$ Hz, $^4J(^{13}\text{C}-^{31}\text{P}) = 2.9$ Hz; C_{3,5}), 132.5 (d, $^2J(^{13}\text{C}-^{31}\text{P}) = 11.2$ Hz; P-Ph_{meta}), 133.0 (d, $^1J(^{13}\text{C}-^{31}\text{P}) = 70.9$ Hz; C_{2,6}), 133.2 (d, $^1J(^{13}\text{C}-^{31}\text{P}) = 87.5$ Hz; C_{2,6}), 134.4 (d, $^4J(^{13}\text{C}-^{31}\text{P}) = 2.9$ Hz; P-Ph_{para}), 134.6 (dd, $^2J(^{13}\text{C}-^{31}\text{P}) = 14.6$ Hz, $^4J(^{13}\text{C}-^{31}\text{P}) = 2.9$ Hz; C_{3,5}), 135.6 (s, $^3J(^{13}\text{C}-^{119}\text{Sn}) = 52.5$ Hz; Sn-C_{meta}), 138.8 (d, $^4J(^{13}\text{C}-^{31}\text{P}) = 2.9$ Hz; Sn-C_{ipso}), 151.3 (dd, $^2J(^{13}\text{C}-^{31}\text{P}) = 27.2$ Hz, 22.4 Hz; C₁), 156.6 (dd, $^3J(^{13}\text{C}-^{31}\text{P}) = 12.6$ Hz, 9.7 Hz, C₄). $^{31}\text{P}\{^1\text{H}\}$ NMR (121.49 MHz, CDCl₃): δ -143.2 (sept, $^1J(^{31}\text{P}-^{19}\text{F}) = 712$ Hz); PF₆⁻), 25.0 (d, $\nu_{1/2}$ 5 Hz, $J(^{31}\text{P}-^{31}\text{P}) = 3.0$ Hz; P=O), 54.8 (d, $J(^{31}\text{P}-^{31}\text{P}) = 3.0$ Hz, ($J(^{31}\text{P}-^{119}\text{Sn}) = 37.1$ Hz); P=S). $^{119}\text{Sn}\{^1\text{H}\}$ NMR (111.92 MHz, CDCl₃): δ -132 (d, $\nu_{1/2}$ 9 Hz, $J(^{119}\text{Sn}-^{31}\text{P}) = 37$ Hz). IR (KBr): $\tilde{\nu}(\text{P}=\text{O})$ 1155 cm⁻¹. Anal. Calcd for C₄₀H₄₅O₃F₆P₃SSn: C, 61.1; H, 5.9. Found: C, 60.4; H, 5.4.

In Situ Generation of 6-tert-Butyl-4-(diphenylphosphinothioyl)-1-isopropoxy-1-oxo-3,3-diphenyl-2,1,3-benzoxaphosphastannole (5). To a solution of **4** (44 mg, 0.047 mmol) in C₂D₂Cl₄ (1.5 mL) was added tetraphenylphosphonium bromide, PPh₄⁺Br⁻ (20.9 mg, 0.05 mmol). After the reaction mixture had been stirred

at 65 °C for 6 h the solution was characterized by NMR spectroscopy. Subsequently, the solvent was removed in vacuo, and the residue was investigated by electrospray mass spectrometry. Attempts at isolating analytically pure compound **5** failed.

$^{31}\text{P}\{^1\text{H}\}$ NMR (81.02 MHz, C₂D₂Cl₄): δ 15.2 (d, $\nu_{1/2}$ 1.6 Hz, $J(^{31}\text{P}-^{31}\text{P}) = 2.0$ Hz, P=O), 51.4 (d, $\nu_{1/2}$ 1.4 Hz, $J(^{31}\text{P}-^{31}\text{P}) = 2.0$ Hz, $J(^{31}\text{P}-^{119}\text{Sn}) = 64.8$ Hz; P=S). $^{119}\text{Sn}\{^1\text{H}\}$ NMR (111.92 MHz, CDCl₃): δ -168 (d, $\nu_{1/2}$ 18 Hz, $J(^{31}\text{P}-^{119}\text{Sn}) = 65$ Hz). ESI-MS: $m/z = 745.1$ ([5-H]⁺ corresponding to natural isotope distribution).

Acknowledgment. We thank the Deutsche Forschungsgemeinschaft for financial support.

Supporting Information Available: For compounds **1-4** details of structure determination, atomic coordinates, bond lengths and bond angles, and displacement parameters in cif format. This material is available free of charge via the Internet at <http://pubs.acs.org>.

OM0600590